

3.0 Experimental and Numerical Methods

Preface

This chapter provides additional information regarding the experimental and numerical methods used for this research. The information contained within is meant to supplement the brief descriptions provided in later chapters (manuscripts) and provide a guide for future Polymer Processing Laboratory personnel.

This chapter presents relevant details regarding the materials studied, the experimental apparatus and procedure followed, and the numerical methods utilized to fulfill the research objectives identified in the previous chapter. Section 3.1 identifies the polyethylene resins that are used during the course of this work. Section 3.2 presents the rheometric test methods used to characterize each of the polyethylene resins. Sections 3.3, 3.4, and 3.5 summarize the experimental apparatus and methods used for the melt fracture analysis, flow visualization, and pressure profiling, respectively. Lastly, section 3.6 will review the hardware and software used for performing numerical simulations as well as the software execution procedure.

3.1 Materials Studied

This work focuses on the rheology and flow behavior of two classes of polyethylene resins. The first class of resins is the crux of this research project and consists of sparsely long-chain branched and linear metallocene-catalyzed polyethylenes (MCPE). These materials are compared and contrasted in order to understand the subtle effects of sparse degrees of long-chain branching on the flow behavior of narrow molecular weight distribution polyethylene resins. The second class of materials includes the "conventional" PE resins. Specifically, highly branched LDPE and strictly linear LLDPE are included in this particular classification. These resins serve as branched and linear controls with which to compare to the MCPE resins, and thus gauge their *processability*.

Table 3.1: Polyethylene Resin Data

<i>Resin</i>	M_w	M_w/M_n	M_z	$LCB / 10^4 C$
Exact 0201	88 700	2.14	158 900	0.79
Exact 3132	111 000	2.04	180 400	—
Affinity PL1840	87 400	2.43	160 200	0.57
Affinity PL1880	115 800	2.12	183 700	0.18
NTX101	122 700	3.44	319 700	—
NA952	235 500	17.1	2 619 300	39 ^a

^a: C^{13} NMR measurement

3.1.1 Metallocene-Catalyzed Polyethylenes

The metallocene-catalyzed polyethylene resins are divided into two groups. The first group consists of sparsely long-chain branched resins and the second consists of strictly linear resins. The reasons for having both groups is to understand the overall significance of long-chain branching on rheology and flow behavior, and to better quantify the sensitivity of flow properties to branch content. All of the MCPE resins analyzed in this study are commercially available resins developed for film blowing applications. Furthermore, none of these film-grade resins contains processing aids or slip/antiblock agents that might alter their inherent melt flow behavior.

All of the MCPE resins have been characterized by researchers at Dow Chemical (Freeport, TX) using high-temperature gel permeation chromatography (GPC) coupled with dilute solution low-angle laser light scattering (LALLS). The theoretical basis for this particular technique can be found elsewhere [Zimm(1949)]. This combined-technique method provides typical molecular weight distribution curves, but also gives an indication of the long-chain branch content. The molecular characteristics of each of the MCPE resins are tabulated in Table

3.1. All of the MCPE resins used in this study have narrow molecular weight distributions (MWD ~ 2), characteristic of metallocene-catalyzed polyolefins.

The sparsely branched MCPE resins contain different degrees of long-chain branching content. They include the Dow Affinity PL1840, Dow Affinity PL1880 and ExxonMobil Exact 0201 resins. The Dow Affinity resins have been produced using the Dow constrained-geometry [metallocene] catalyst (CGC) technology spoken of in Section 2.1, while the Exact resin has been produced using the EXXPOL® catalyst technology. Table 3.1 shows that the Affinity PL1880 resins contains the lowest branch content of the three resins at 0.18 LCB/10000 carbons, but has the highest weight-averaged molecular weight (M_w) at 115,800 g/mol. Conversely, the Exact 0201 resin has the highest branch content at 0.79 LCB/10⁴ carbons, yet one the lowest M_w . The Affinity PL1840 is similar in molecular weight to the Exact 0201 resin, but has an intermediate degree (0.57 LCB/10⁴ carbons) of long-chain branching. All of the branched MCPE resins described are ethylene-octene copolymers.

The linear MCPE resin used for this study is the Exact 3132 resin. Exact 3132 is manufactured using the EXXPOL® catalyst technology. The linear MCPE resin has been characterized in a similar manner to the branched MCPE resins and the results can be found in Table 3.1. The molecular analysis confirms that no long-chain branches are present, as expected. The molecular weight and MWD are similar in value to the branched Affinity PL1880 resin. Finally, the Exact 3132 resin is an ethylene-hexene copolymer.

3.1.2 Conventional Polyethylenes

In addition to the MCPE resins, a set of conventional polyethylene resins has been investigated. The conventional resins include a high-temperature, high-pressure autoclave

produced low-density polyethylene (LDPE) manufactured by Equistar, and a Ziegler-Natta polymerized ethylene-hexene copolymer produced by ExxonMobil. The conventional LDPE is commercially designated as NA952 and has a melt flow index of 2.0; the conventional LLDPE is commercially designated as NTX101 and has a melt flow index of 0.9. Furthermore, the molecular characteristics of each of these resins can also be found in Table 3.1. Neither resin has processing aids nor slip/antiblock agents that might obscure their true melt flow behavior. Although these resins represent more complex fluids, with broader molecular weight distributions than the MCPE resins, they embody the typical responses of branched and linear polyethylenes, respectively. Therefore, these conventional resins will serve as experimental controls with which to compare the branched and linear MCPE resins.

3.2 Rheological Characterization

In order to realize the effects arising from molecular structure, and more specifically from long-chain branching, the rheological properties of these resins must first be measured. Rheological characterization is generally divided into two separate flow kinematics: shear and shear-free flows. The kinematic arguments and relevant equations are presented earlier (Section 2.2.1). In this section, the apparatus used to perform rheological measurements and the operating procedures used to acquire kinematic specific data will be presented.

3.2.1 Shear Rheology

The shear rheological measurements can be further divided into two categories. These two categories are homogeneous and nonhomogeneous shearing flows. Homogenous flows are characterized by deforming stresses that are independent of position, while nonhomogeneous

flows exhibit spatial dependence. This comparison is the same as that between drag flows and pressure-driven flows. In this study, a torsional rheometer has been used to obtain homogeneous rheological data and a capillary rheometer has been used to obtain nonhomogeneous rheological data. Although both methods provide shear viscosity, the versatility and range of data available differs.

Torsional Rheometry

Steady shear and small-amplitude dynamic oscillatory experiments are performed using a Rheometrics Mechanical Spectrometer Model 800 (RMS-800). The RMS-800 is a controlled strain torsional rheometer capable of steady angular rotation and dynamic oscillatory displacements. A dual range force rebalance transducer (FRT) is used to measure both torque and normal force response during testing. Each test is performed within an inert nitrogen environment using cone-and-plate test fixtures having a plate diameter of 25mm and a cone angle of 0.1 radians. This particular configuration provides the most accurate rheological data due to the homogeneous deformation field.

The RMS-800 provides viscoelastic data in the range of 0.001 to 100 s⁻¹. Steady shear deformation provides shear viscosity (η) and primary normal stress difference (N_1) data in the range of 0.001 to 1.000 s⁻¹. Small-strain dynamic oscillatory deformations provide complex viscosity (η^*), storage modulus (G'), and loss modulus (G'') data in the range of 0.1 to 100 rad/s. In most cases, the Cox-Merz rule has been assumed to hold true ($\omega = \dot{\gamma}$).

Capillary Rheometry

Nonhomogeneous steady shear experiments at shear rates greater than 10 s^{-1} are performed using a Goettfert Rheograph 2001 (RG2001). The RG2001 is a controlled displacement capillary rheometer capable of volumetric displacements of $3.5 \text{ cm}^3/\text{s}$ and applied loads of 20 kN. The dies used for rheological analysis are tungsten carbide steel capillaries with die diameters of 1 mm and lengths of 10, 20, and 30 mm. Furthermore, each of the dies has a 180° included entry angle (flat entrance) and a barrel-to-capillary contraction ratio of 15.

The RG2001 provides steady shear viscosities (η) in the range of 10 to 1000 s^{-1} . Because of the nonhomogeneous flow field the steady state shear viscosity is the only relevant quantity. The limits of accuracy are determined by the sensitivity of the mounted pressure transducer at low rates and the onset of melt fracture at high rates. Due to the large contraction ratio, a Bagley end analysis is typically performed to correct the effects of entrance pressure loss on the wall shear stress and shear viscosity. Furthermore, the Rabinowitsch correction is also utilized to correct for non-parabolic flow profiles within the capillary.

3.2.2 Extensional Rheology

Uniaxial extensional measurements are carried out using a Rheometrics Extensional Rheometer Model 9000 (RER-9000). The RER-9000 is based on the original design by H. Munstedt (1979) in which a homogeneous molded cylindrical sample is suspended in a heated oil bath and fixed between a stationary platform and a mobile drawing arm. Figure 3.1 represents a basic schematic of the device. The density of the oil (Dow Corning Fluid 200) is so chosen to match the resin density at the test temperature, therefore creating a neutrally buoyant environment. The applied force resulting from deformation is measured using a linear variable

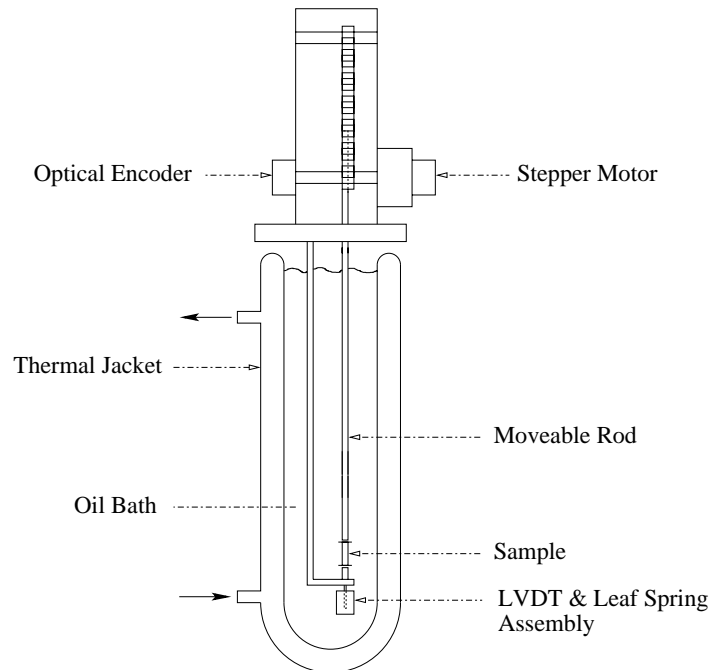


Figure 3.1: RER9000 Schematic

differential transformer (LVDT). A viewing window is used to assure that homogeneous deformation of the sample occurs.

The RER-9000 provides homogeneous uniaxial deformation at a specified applied strain rate or stress. The instrument is capable of applying extensional strain rates from 0.001 to 5 s^{-1} , however the practical limit is generally found to be 1 s^{-1} . The maximum strain, using 22 mm samples, is typically found to be 3.0 strain units. Because the presence of a free surface often leads to nonhomogeneous or nonuniform deformation, many duplicate tests are performed. Those samples that "appear" to deform uniformly are averaged to obtain a statistical response for a given strain rate and strain.

3.3 Melt Fracture Analysis

The experiments examining the melt fracture behavior of metallocene and conventional polyethylene resins were found to require two key components. The first component consists of

a pumping device capable of accurately metering polymer melt at a desired flow rate. The second component is an imaging device that can resolve both gross and fine features of extruded samples. In the following section, the chosen apparatus and operating procedures used to perform the melt fracture studies will be outlined.

3.3.1 Apparatus

The Goettfert Rheograph 2001 (RG2001) capillary rheometer (see Section 3.2.1) was chosen as the metering device for this study. The RG2001 is a positive displacement pump that provides very accurate metering of polymer melt through round capillary dies. The RG2001 is fitted with a pre-contraction pressure transducer port that is used to measure transient and steady-state driving pressures. Additionally, a high-speed data acquisition system consisting of a 12-bit A/D acquisition card (Model ADM12-11) by Quatech and an IBM-compatible personal computer (PC) are utilized to rapidly measure pressure fluctuations during slip-stick flow conditions.

The imaging device chosen for this study is either a Cambridge Instruments Stereoscan Model 200 scanning electron microscope (SEM) or a Leo 1550 field emission scanning electron microscope (FE-SEM). An SEM was found to be most versatile because it can provide both coarse and fine resolution micrographs of the extruded melt fracture samples. Furthermore, scanning electron microscopy provides greater image contrast than optical microscopy when imaging semi-transparent materials like polyethylene.

3.3.2 Operating Procedure

In the next two subsections, detailed instructions for obtaining and imaging melt fracture specimens using the apparatus described earlier are provided.

Sample Collection

1. Prepare the Rheograph 2001 for operation according to the instrument user manual. This step includes setting the operating temperature, installing the capillary die, and installing and calibrating the pressure transducer.
2. Enter the desired piston rate (0.0001 to 20 mm/s) and activate the servo-hydraulic system.
3. Allow the driving pressure to equilibrate. If unsteady flow conditions occur, attach the high-speed data acquisition system to the chart recorder input leads and capture the sinusoidal pressure response.
4. Obtain multiple samples of the extrudate and quench in water.
5. Document the extrusion temperature, capillary dimensions, and pressure reading for each sample collected.
6. Repeat steps 2-5 for each subsequent piston rate.
7. Repeat steps 1-6 for each extrusion capillary used.

Imaging

1. Securely mount each sample onto a separate specimen stage using conductive tape.
2. Sputter coat the specimens with 10nm thick layer of gold.

3. Prepare the Leo 1550 for operation according to the instrument user manual. This step includes mounting the specimen stages, evacuating the imaging chamber, and positioning each specimen stage for imaging.
4. Obtain micrographs at 20x & 50x magnification.
5. Label the micrograph(s) appropriately and document relevant imaging parameters.
6. Repeat steps 4-5 for each melt fracture specimen.

3.4 Flow Visualization

The flow visualization experiments are very complex studies that consist of a large number of components and require precise measurement of experimental quantities. The current section will provide an overview of the apparatus and operating procedure used to obtain isochromatic fringe patterns and particle streak patterns.

3.4.1 Apparatus

The flow visualization studies rely upon three key component systems: the polymer delivery system, the visualization die, and the optical imaging system. The following three subsections will summarize the individual devices that make up the component systems.

Polymer Delivery System

The polymer delivery system has been designed to provide pulseless, precisely metered molten polymer at near isothermal conditions. This is accomplished using a 25.4mm plasticating laboratory extruder (Killion) and 1.752 cc/rev gear pump (Zenith, HPB-5556). The gear pump is driven by a 1/4 horsepower AC motor (US Electric Motors) that operates between 11 and 113

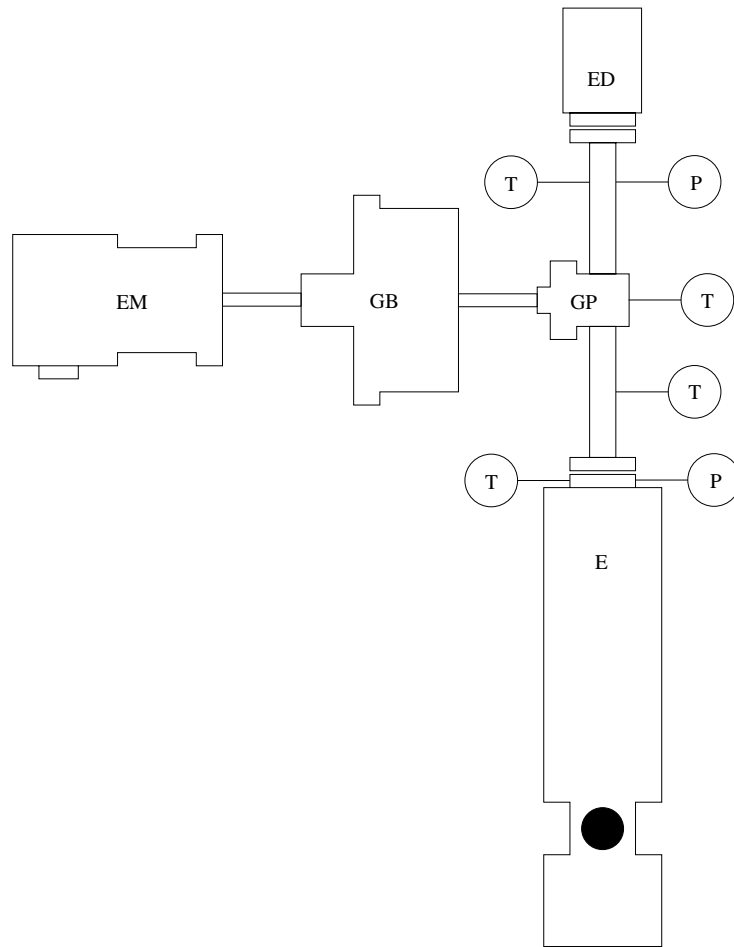


Figure 3.2: Polymer Delivery System. E – Extruder, GP – Gear Pump Assembly, EM – Electric Motor, GB – Gearbox Reducer (optional), ED – Extrusion Die, T – Temperature Probe, P – Pressure Probe.

rpm. Lower flow rates are obtained by placing a gear-reducing unit (Reynolds Ltd.) between the motor and gear pump. The gear reduction ratio is 21.4:1. High-pressure conduit connects the extruder and gear pump assemblies while a high-pressure conduit fitted with a Kenics static mixer connects the gear pump to downstream equipment. The static mixing element is used to thermally and mechanically homogenize the polymer melt.

The primary operating variables are flow rate and melt temperature. The flow rate is manually adjusted by first varying the gear pump drive speed and then adjusting the extruder screw speed to maintain acceptable back pressure on the gear pump inlet. An optical tachometer

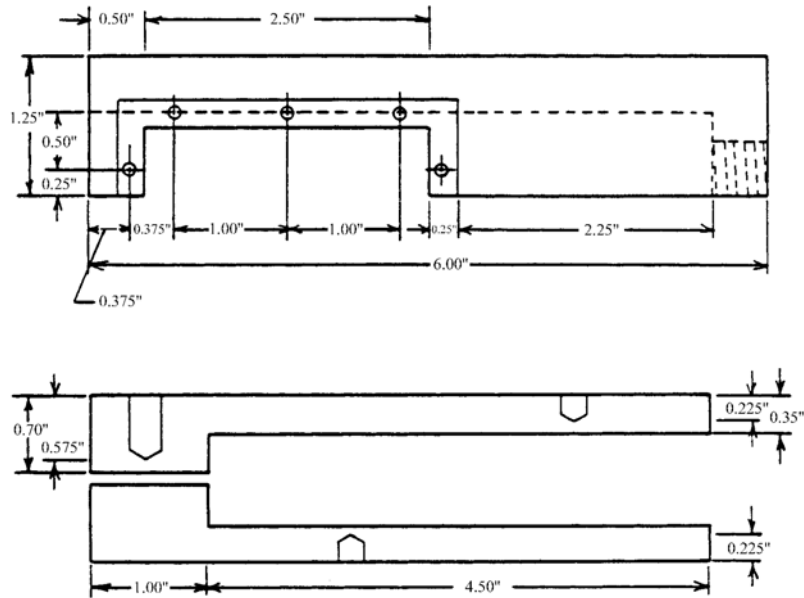


Figure 3.3: Visualization die schematics [White (1987)].

is linked to the gear pump drive shaft to determine the volumetric flow rate. The melt temperature is controlled by 4 sets of heating elements. The first set is found in the extruder, the second on the extruder-gear pump connecting conduit, the third on the gear pump assembly, and the fourth on the static mixer assembly. All four regions are regulated around a desired set point via PID controllers.

Visualization Die

The visualization die used for this study is a planar contraction die originally designed and constructed by S. White [White (1987)]. The basic features and dimensions of the die are found in Figure 3.3. The die is machined from 316 stainless steel and features insert slots that can be used to vary the contraction geometry. This study employs the previously machined 8:1 planar contraction geometry inserts. The upstream slit dimensions are 25.4 x 20.3 x 114.3 mm (WxHxL) and the downstream slit dimensions are 25.4 x 2.54 x 25.4 mm. The machining

tolerance is 0.026mm. Heating of the die is accomplished using three, independently controlled sets of strip resistance heaters (Industrial Heater Co.).

The most unique features of the visualization die are the optical windows. Two rectangular windows are positioned on opposite sides of the contraction region. The optical windows are made from commercial grade quartz (Dell Optics) and have dimensions of 25.4 x 31.7 x 63.5 mm (WxHxL). The thickness was specifically chosen to withstand the large hydrostatic pressures present at high flow rates. The windows are secured using silicone gasket material and steel retaining brackets.

Optical Imaging System

The optical system is used to *illuminate* the flow field. The specific attributes and components are determined by the particular study. For flow birefringence studies, the generation of isochromatic fringe patterns requires a monochromatic light source, polarization optics, and imaging device [Janeschitz-Kriegl (1983)]. The monochromatic light source chosen for this study is an unpolarized 0.5 mW He-Ne laser (Spectra Physics). The characteristic wavelength is 632.8 nm. Because the beam diameter is only 0.9mm, it is expanded using a 10x objective lens (Tower) and 76.2 mm collimating lens (Oriel). The expanded beam is then passed through a "polarizer" with its optic axis rotated 45 degrees from the flow direction. The polarized beam passes through the visualization die and proceeds through the "analyzer". The analyzer is a matched polarizing optic with its optic axis orthogonal to the "polarizer". The resulting beam is then focused using a 76.2 mm focusing lens (Oriel) and imaged using a digital camera (Sony TRV900). All optic components are mounted to an optic rail to maintain alignment.

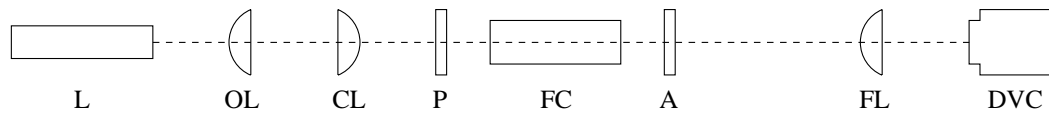


Figure 3.4: Optial Rail Assembly. L – Laser, OL – Objective Lens, CL – Collimating Lens, P – Polarizer (Plane or Circular), FC – Flow Cell, A – Analyzer (Plane or Circular), FL – Focusing Lens, DVC – Digital Video Camera.

The “polarizer” and “analyzer” can be either plane or circular polarizers. Plane polarizers simply polarize the incident beam along the optic axis. Plane polarization gives rise to dark field patterns which represent whole order fringes ($N=0,1,2,\dots$). On the other hand, circular polarization combines a plane polarizer with a quarter wave plate. This combination yields a retarded wave and gives rise to light field patterns which represent half order fringes ($N=1/2, 3/2, 5/2, \dots$). The mathematical details pertaining to flow birefringence can be found in Appendix G.

The particle streak patterns are produced using a much simpler setup. White light illuminates the flow cell at a 45 degree angle and reflects off of solid particles dispersed in the melt stream. These particles are generated by adding 0.5% by weight of powdered nickel or iron to the extruder feed. Generally, a small amount of mineral oil is added to better disperse the powdered metal and prevent settling in the extruder throat. A digital camcorder (Sony TRV900) is used to record the streaming particles. The recorded flow patterns are then manipulated using Adobe Photoshop 5.0 to obtain time-lapsed streak patterns.

3.4.2 Operating Procedure

In the next three subsections, detailed instructions for obtaining isochromatic fringe patterns and particle streak patterns are provided. A procedure common to both experiments will be provided first, followed by experiment specific instructions.

System Initialization

1. Turn on extruder and temperature controllers.
2. Set temperature setpoints and allow one hour soak time.
3. Set the zero and gain (80\% scale) of all pressure transducer indicators.
4. Feed polymer pellets into the extruder hopper and initiate screw rotation at 10 rpm.
5. Once considerable backpressure is observed (~1000 psi), reduce screw speed and initiate gear pump motor (setting 0).
6. Bring gear pump motor to desired speed and adjust extruder screw speed to maintain 1000 psi back pressure on extruder pressure transducer.
7. Allow 30 minute purge period to remove resident polymer melt.

Isochromatic Fringe Patterns

8. Install and align the optic components as illustrated in Figure 3.4. Assure that the expanded, collimated beam is centered around the contraction entrance along the neutral flow axis (z-axis).
9. Obtain dark field stress patterns by placing the plane polarizers along the optical rail. Insure that the polarization axes are crossed.
10. Replace the plane polarizers with the circular polarizers and obtain the light field pattern. Insure that the quarter wave plates are facing each other and that the polarization axes remain crossed.
11. Repeat steps 8 and 9 for each flow rate.
12. Extract still images for each flow rate using digital video software (MiroVideo 200).

Particle Streak Patterns

8. Add the powdered metal tracers to the feed polymer and allow sufficient time for complete dispersal of tracer particles across the viewing region.
9. Align the digital video camera with the visualization die and orient the light source to get maximum reflection and contrast of the embedded tracer particles.
10. Record the flow from 5 to 20 minutes, depending on the imposed flow rate.
11. Repeat step 9 for each flow rate.
12. Extract the full motion video for each flow rate and generate streak patterns using image manipulation software.

3.5 Pressure Profiling

The pressure profiling studies investigate the effects of an abrupt planar contraction on the flow behavior of polyethylene melts. Specifically, the observed pressure drop along the flow axis will be measured. The following section will summarize the key components of the apparatus used, and the operating procedure used to perform the studies.

3.5.1 Apparatus

The pressure profiling apparatus is similar to that of the flow visualization studies. The same polymer distribution system described previously is also used for metering polymer melt to pressure profiling die. The main difference is that of the extrusion die utilized. The profiling die was fabricated specifically for this study. The relevant dimensional schematics can be found in Figures 3.5 and 3.6. The profiling die is machined from 440C stainless steel and consists of six pressure transducer ports machined along the slit flow path. Four of these ports are placed

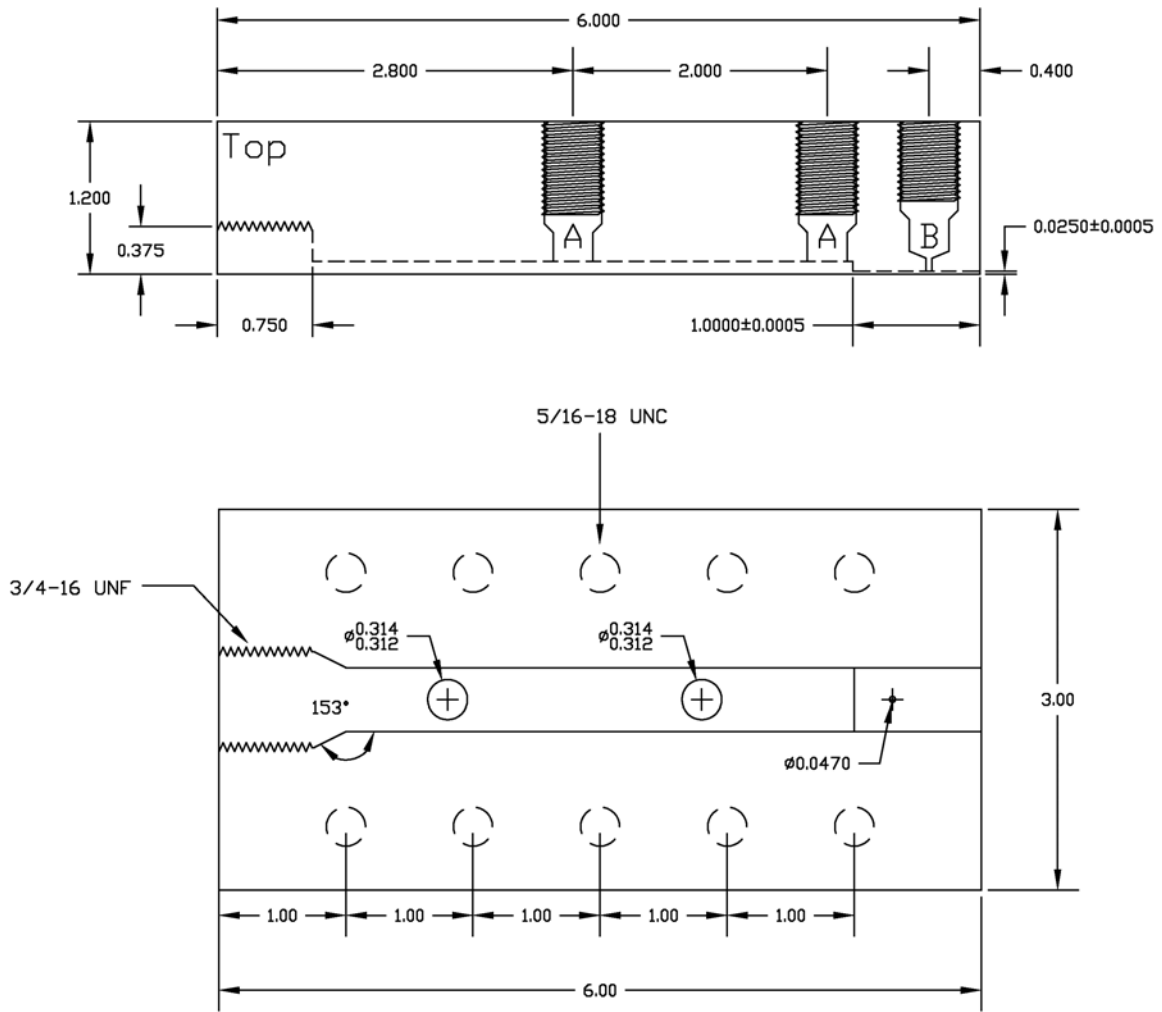


Figure 3.5: Profiling Die (Top half)

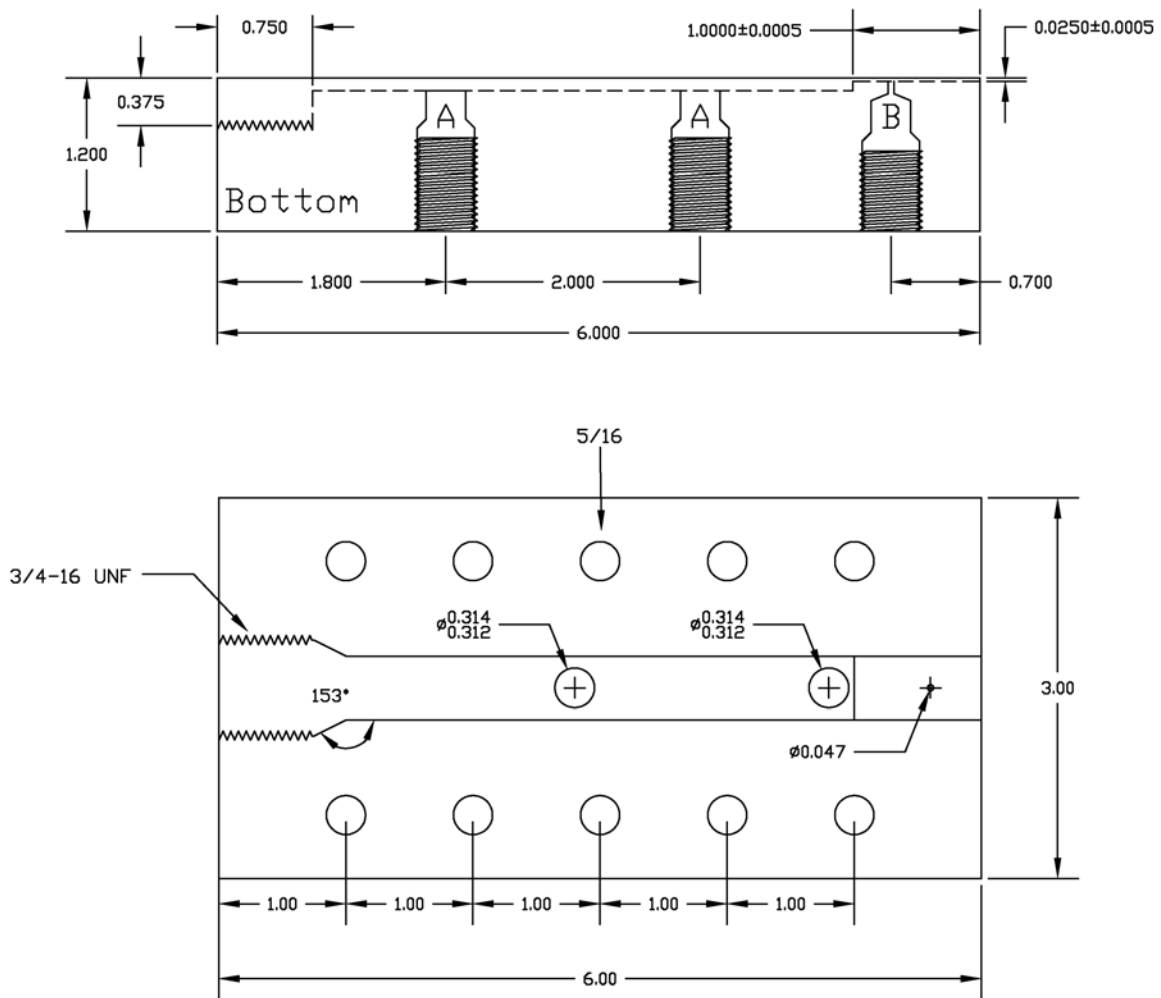


Figure 3.6: Profiling Die (Bottom Half)

upstream of the abrupt 4:1 planar contraction, the remaining two ports are found downstream. The upstream slit dimensions are 12.7 x 2.54 x 108.0 mm (WxHxL) and the downstream dimensions are 12.7 x 0.635 x 25.4 mm (WxHxL). These dimensions were chosen in order to augment the maximum achievable shear rate to approximately 100 s^{-1} .

The pressure measurements were obtained using melt pressure transducers (Dynisco PT422A) with maximum pressure ranges from 34.5 to 103.4 bars (500 to 1500 psi). Calibration of these transducers was performed using a dead weight tester (Model No. 23-1) manufactured by Chandler Engineering (Tulsa, OK). Practical pressure measurements were obtained using scaled pressure indicators (Dynisco ER478) or the Quatech A/D data acquisition card described earlier.

Temperature control of the die is accomplished using two enclosing aluminum heating plates that are securely fastened to the top and bottom faces of the die. The aluminum plates have been pre-drilled to accept twelve 150W 6.35 x 38.1 mm (0.25 x 1.5 in.) cartridge heaters. Combined with appropriate temperature controllers (Omega CN9000), these heating plates provide near isothermal flow conditions within the profiling die.

3.5.2 Operating Procedure

The current subsection provides instructions for initializing the polymer delivery system, preparing the profiling die for use, and obtaining pressure measurements during operation.

System Initialization

1. Turn on extruder and temperature controllers.
2. Set temperature setpoints and allow one hour soak time.

3. Set the zero and gain (80\% scale) of all pressure transducer indicators.
4. Feed polymer pellets into the extruder hopper and initiate screw rotation at 10 rpm.
5. Once considerable backpressure is observed (~1000 psi), reduce screw speed and initiate gear pump motor (setting 0).
6. Bring gear pump motor to desired speed and adjust extruder screw speed to maintain 1000 psi back pressure on extruder pressure transducer.
7. Allow 30 minute purge period to remove resident polymer melt.

Pressure Measurements

8. While the polymer distribution system components are heating: attach the heating plates, install the pressure transducers, and initiate heating of the profiling die. Allow a one-hour soak and then set the zero and gain (80% scale) for all pressure transducer indicators.
9. During operation, record the indicated pressure for each of the six melt transducers.
10. Repeat step 9 for each subsequent flow rate.

3.6 Numerical Simulations

Numerical simulations are performed to assess the ability to predict the flow behavior of the metallocene and conventional polyethylene resins under complex flow conditions. The computational method and capacity greatly determine the practical limits of computational efficiency. In the following subsections, the hardware and software packages used to perform numerical simulations, and the numerical procedure used to obtain flow predictions are summarized.

3.6.1 Hardware & Software

All of the numerical simulations undertaken in this project were performed using a Silicon Graphics Inc. (SGI) Origin 200 server. The Origin 200 is a deskside, entry level workgroup server supporting one to four MIPS processors. Currently, the Origin 200 is fitted with two 270 MHz IP27 RISC processors and 512 MB of main memory. The installed 64-bit operating system is IRIX 6.5.10f. In addition to the numerical simulations, the curve and parameter fitting calculations are performed using a personal Pentium III 733 MHz computer.

The software used for this study can be divided between two classifications, parameter fitting applications and finite element method simulations. The parameter fitting software is self-written and coded in the Fortran 90 conventions. Absoft Pro Fortran 6.0 (academic) is used to compile the source code into an executable format. Fitting programs for the Generalized Newtonian Fluid (GNF), Phan-Thien and Tanner (PTT) and McLeish-Larson Pom-Pom models have been written. Furthermore, IMSL numerical subroutines, available from Visual Numerics, are used to solve ordinary and partial differential equations as well as numerical integration calculations. A complete listing of all relevant Fortran 90 source code is found in Appendix D.

The finite element method simulation software used for this study is Polyflow 3.8 (Fluent). This particular version is written for the IRIX operating system and therefore used on the SGI Origin 200 server. The Polyflow 3.8 software suite consists of four discrete applications: GAMBIT, Polydata, Polyflow, and FIPost. The GAMBIT application is used to define and mesh the desired flow region. Polydata is used to specify simulation parameters: the flow boundary conditions, the chosen constitutive equation, the interpolation techniques, and local and global convergence criteria. Polyflow is the finite element method solver and actually

performs the simulation calculations. The final application, FIPost, is a postprocessor application and provides visualization of the simulation results in a convenient, graphical manner.

3.6.2 Procedure

The procedure used for obtaining accurate numerical simulations does not follow a strict “operating procedure”, but rather a methodology. In this section, a *method* for performing numerical simulations that are derived from physical experiments and calculated from available rheological data is outlined. Although this approach may not be deemed the most accurate or the most efficient, it has been determined to be the most consistent one across many different fluid descriptions.

Parameter Fitting

Parameter fitting is arguably the most important step involved in obtaining accurate numerical predictions. It is during this step that experimentally measured data is translated into a considerably smaller set of constitutive parameters. Therefore, it is very important to understand the flow kinematics and range of applicability associated with the rheological measurements in comparison to that of the simulated geometry. Excessive extrapolation of rheological properties beyond experimentally measured bounds may lead to significant inaccuracies in the resulting numerical predictions.

The parameter fitting method consists of three steps. The first step is fitting available linear viscoelastic data to obtain the discrete relaxation spectrum. Linear viscoelastic data is usually comprised of G' , G'' , and η in the zero-shear viscosity plateau. The discrete relaxation spectrum, composed of a finite number of relaxation times and strengths, is calculated using the

fitting programs. The general rule of thumb is one relaxation time per decade of data. The fitting algorithms implement non-linear least squares minimization to obtain the relaxation strengths at each user-supplied relaxation time.

The second step involves the fitting of the nonlinear shear parameters found within each of the constitutive equations investigated. Because all of the parameters in the GNF model are nonlinear shear parameters, nonlinear regression is used to obtain the model parameters by reducing the sum of the squared errors. For the PTT model, the ξ parameter is the nonlinear shear parameter, while for the Pom-Pom model τ_s is the respective nonlinear parameter. The difference between each of these parameters is the source of rheological data used for fitting. ξ is generally determined from manual shifting of $\eta(\dot{\gamma})$ to overlay on $\eta'(\omega)$ data. Therefore numerical fitting is not utilized. τ_s is significantly more difficult to obtain from shear data alone and is often determined with the use of extensional data as well. The combination of the nonlinear shear parameter and discrete relaxation spectrum provides more accurate predictions during *pure* shear deformations.

The final step is fitting extensional viscosity growth data to obtain the shear-free parameter. For the PTT model, ε is the nonlinear shear-free parameter, while for the Pom-pom model, q is the nonlinear shear-free parameter. In addition to the relevant rheological data, the use of the discrete relaxation parameter and non-linear shear parameters is also required. Because of the strain-hardening nature of branched PE resins, it is very difficult to obtain steady extensional viscosities. Therefore, most of the available data is transient extensional viscosity data.

Polyflow Simulations

The Polyflow numerical simulations follow a very straightforward method for performing finite element method calculations on user-defined flow domains. As mentioned in the "Hardware & Software" section, there are four discrete applications used to setup, execute, and analyze the numerical simulations. Figure 3.7 illustrates the process for carrying out numerical simulations using the Polyflow software suite. A comprehensive description of each application can be found in the respective Polyflow manuals [Polyflow (1998)].

The first application is the GAMBIT mesh generation package. This software application generates two- or three-dimensional, structured or unstructured, finite element meshes. Furthermore, triangular or quadrilateral element geometries are available for 2-D meshes. The user-supplied information includes the mesh dimensions and boundary types. The resulting mesh file is known as a GAMBIT neutral (NEU) file. This mesh file is utilized by the Polydata software application.

The next user-activated application is Polydata. Polydata is used to specify simulation parameters, including: boundary conditions, constitutive equations, variable interpolation techniques, and convergence criteria. Polydata uses the NEU mesh file described above and converts it to a Polyflow compatible MSH file. Polydata then uses this mesh file to map appropriate boundary conditions. The simulation data file (DAT) produced by Polydata is then used as primary input for the finite element solver, Polyflow.

Polyflow is the actual FEM solver. This software application uses the Polydata DAT file as input and generates various output files. The primary outputs are the Fluent mesh (FLUM) and Fluent result (FLUR) files. These files contain the nodal solutions for each independent variable (pressure, velocity, and stress). Furthermore, the Fluent output files are also output for

each evolutive step of the simulation. This is very useful for analyzing the flow development as a function of flowrate or viscoelastic character. Optionally, result probe files (PRB) can be used to monitor variable values at specific locations or nodes within the flow geometry.

The final application is the simulation postprocessor, FIPost. FIPost uses the Fluent output files from Polyflow to visualize the results. FIPost provides pressure, velocity, stress, and streamline contours across the flow domain. These contour patterns can be saved in a graphic format (EPS, TIFF) or printed for future use. Additionally, nodal values can be plotted and/or saved to disk for later use as well.

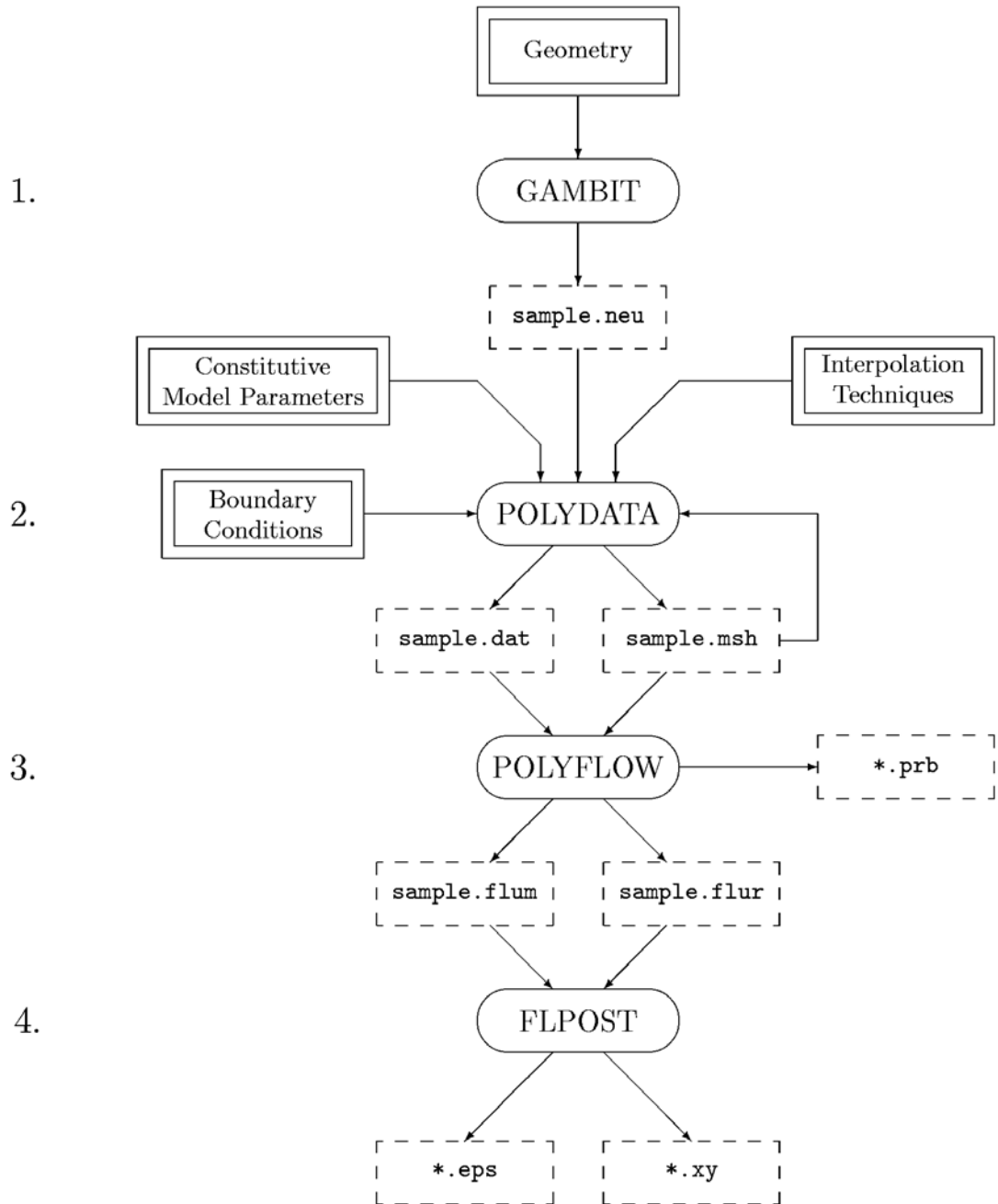


Figure 3.7: Polyflow Simulation Procedure

3.7 References

Janeschitz-Kriegl, H., *Polymer Melt Rheology and Flow Birefringence*, Springer-Verlag, New York, 1983.

Münstedt, H., *J. Rheol.*, **23**, 421 (1979).

Polyflow S.A., Belgium, *Polyflow 3.8*, 2000.

White, S.A., *The Planar Entry Flow Behavior of Polymer Melts: Experimental and Numerical Analysis*, Ph.D. Dissertation, Virginia Tech, Blacksburg, VA, 1987.

Zimm, B.H. and H.W. Stockmayer, *J. Am. Chem. Soc.*, **17**, 1301 (1949).